Science and Technology Indonesia
e-ISSN:2580-4391 p-ISSN:2580-4405
Vol. 11, No. 3, July 2026

Research Paper

Structural Modification of Bentonite by Rice Husk Biochar for Enhanced Methylene Blue Removal under Visible Irradiation

Neza Rahayu Palapa[1*], Elsa Irma Esthomihi Manurung[1], Yulizah Hanifah[2], Davin Philo[3]

[1]*Department of Chemistry, Faculty of Mathematic and Natural Sciences, Universitas Sriwijaya, Ogan Ilir, South Sumatra, 30662, Indonesia*
[2]*National Research and Innovation Agency, PUSPIPTEK, South Tangerang, Banten, 15311, Indonesia*
[3]*Research Center for Photonics, National Research and Innovation Agency, South Tangerang, Banten, 15314, Indonesia*
***Corresponding author**: nezarahayu@mipa.unsri.ac.id

Abstract
The development of sustainable and low-cost materials for wastewater treatment remains an important environmental challenge. In this study, a bentonite-biochar (Bnt–Bc) composite was prepared through structural modification of bentonite using rice husk–derived biochar followed by KOH-assisted activation. The physicochemical properties of the materials were systematically characterized using XRD, BET, FTIR, SEM, and UV–Vis diffuse reflectance spectroscopy. The results revealed that biochar incorporation modified the interlayer structure of bentonite, resulting in reduced crystallinity, pore structure alteration, and the introduction of additional oxygen-containing functional groups. These structural changes contributed to improved surface reactivity and enhanced interaction with dye molecules. The performance of the materials was evaluated for methylene blue (MB) removal under Visible Light irradiation. The Bnt–Bc composite exhibited significantly higher removal efficiency compared to pristine bentonite and biochar, achieving up to 98% MB removal within 150 min. Kinetic analysis indicated that the removal process followed a pseudo-first-order model. The enhanced performance is attributed to the combined effects of improved adsorption capacity, surface functional groups, and photo-assisted degradation under Visible Light irradiation. This study demonstrates that biochar-modified bentonite composites derived from agricultural waste represent a promising and environmentally friendly material for dye-contaminated wastewater treatment.

Keywords
Bentonite–Biochar Composite, Rice Husk Biochar, Methylene Blue Removal, Visible-Assisted Degradation, Wastewater Treatment

Received: 31 January 2026, Accepted: 21 April 2026
https://doi.org/10.26554/sti.2026.11.3.972-981

1. INTRODUCTION

Clay minerals play a crucial role in environmental remediation due to their layered structures, high cation exchange capacity, surface reactivity, and chemical stability (Banat et al., 2009). Among them, bentonite has been extensively investigated as an effective adsorbent for the removal of dyes and organic contaminants from wastewater, particularly cationic dyes such as methylene blue (MB) (Gnanamozhi et al., 2023; Yontar et al., 2022; Zahara et al., 2023). However, the removal performance of pristine bentonite is predominantly governed by physical adsorption and ion exchange processes, which limits its ability to achieve complete degradation or mineralization of pollutants.

Photocatalytic degradation has emerged as a promising strategy to overcome these limitations by enabling the breakdown of organic molecules into less harmful species under light irradiation (Bopape, 2026; MacHale et al., 2021). To date, most clay-based photocatalytic systems reported in the literature rely on the incorporation of conventional semiconductor materials, such as TiO_2 (Janani et al., 2021; Qian et al., 2018; Xu and Ma, 2021), ZnO (Chakrabarti and Dutta, 2004), or metal oxides (Janani et al., 2021; Saravanan et al., 2013), onto clay surfaces to impart photocatalytic functionality. While such hybrid systems show improved degradation efficiencies, they often suffer from drawbacks including complex synthesis routes (MacHale et al., 2021), potential metal leaching (Dhila et al., 2025), light-shielding effects, and reduced sustainability (Ashamary et al., 2025).

In parallel, biochar derived from agricultural residues has gained increasing attention as a carbonaceous material with abundant surface functional groups, tuneable porosity, and strong adsorption capacity (Kambo and Dutta, 2015). Rice husk biochar, in particular, is rich in silica and oxygen-containing functional groups, making it a promising candidate for interaction with clay minerals. Nevertheless, biochar alone exhibits limited photocatalytic activity and is typically employed only as

an adsorbent or as a support for semiconductor catalysts (Abdu et al., 2025; Zhou et al., 2024).

Recent studies have suggested that structural modification of clay interlayers using organic or carbon-based materials can significantly alter textural properties (Ramesh and Raghavan, 2025), surface chemistry, and mass transfer behaviour (Liu et al., 2024). Despite this potential, the use of biomass-derived biochar to directly modify bentonite interlayers for photo-assisted dye degradation without the addition of conventional semiconductor photocatalysts remains largely unexplored. In particular, the relationship between interlayer modification (Zhao et al., 2026), pore evolution, surface functional groups (Sewu et al., 2019), and photocatalytic performance has not been systematically addressed (Ramesh and Raghavan, 2025).

In this study, we demonstrate that interlayer-modified bentonite using rice husk biochar can act as an efficient semiconductor-free photocatalytic material for methylene blue degradation through a synergistic adsorption–photocatalysis mechanism. The rice husk biochar–bentonite (Bnt–Bc) composite was synthesized via impregnation and chemical activation, and its structural, textural, and surface properties were investigated using XRD, BET, and FTIR analyses. The photocatalytic performance toward MB degradation under irradiation was systematically evaluated and compared with pristine bentonite and biochar. The findings provide new insights into clay–carbon interactions and highlight the potential of sustainable clay-based composites for advanced wastewater treatment applications.

2. EXPERIMENTAL SECTION

2.1 Chemicals and Instruments

Methylene blue (Merck), potassium hydroxide (KOH, Sigma-Aldrich), and bentonite (Merck) were used as received without further purification. Deionized water (Bratachem) was employed throughout the experiments, while rice husk was collected from paddy fields in Ogan Ilir, Indonesia, and used as the biomass precursor for biochar preparation. The concentration of methylene blue was measured using a Thermo Scientific Genesys 150 UV–Vis spectrophotometer. Structural and physicochemical characterizations were carried out using a Shimadzu Prestige-21 Fourier Transform Infrared (FT-IR) spectrophotometer, a Rigaku MiniFlex 600 X-ray diffractometer (XRD), and a Jasco V-760 UV–Vis diffuse reflectance spectrophotometer (UV-DRS, 200–800 nm). Textural properties were determined via N_2 adsorption–desorption analysis using a BELSORP-miniX Brunauer–Emmett–Teller (BET) surface area analyser. Surface morphology was examined by scanning electron microscopy (SEM) using a Hitachi SU3500 instrument at a magnification of up to 5000×.

2.2 Preparation of Rice Husk Biochar and Bentonite–Biochar Composite

The preparation of the composite material was adapted from the method reported by Liu et al. (2024) with minor modifications in the bentonite composition. Rice husk was first thoroughly washed with deionized water to remove adhering impurities, followed by air-drying under sunlight until completely dry. The dried rice husk was then further dehydrated in an oven at 100°C for 48 h to ensure complete removal of residual moisture. Subsequently, the dried rice husk was subjected to pyrolysis at 500°C for 2 h under a continuous flow of nitrogen (N_2) atmosphere to prevent oxidation and ensure an inert environment, resulting in the formation of rice husk biochar.

For the impregnation process, 10 g of rice husk biochar was mixed with 10 g of bentonite and 40 g of KOH. The mixture was dispersed in 500 mL of deionized water and stirred until a homogeneous suspension was obtained. The suspension was then maintained at room temperature for 24 h to promote adsorption and intercalation between biochar and bentonite. After impregnation, the mixture was dried in an oven at 105°C until a constant weight was achieved, yielding the bentonite–biochar composite.

2.3 Evaluation of Methylene Blue Removal under Visible Light Irradiation

Evaluation of Methylene Blue (MB) Removal under Visible Light irradiation was conducted using the bentonite–biochar (Bnt–Bc), Biochar (Bc) and Bentonite (Bnt) composite as the catalyst. Prior to irradiation, all suspensions were magnetically stirred in the dark for 30 min. The effect of catalyst dosage was investigated by adding 25–250 mg of Bnt–Bc to 25 mL of MB solution (50 mg L^{-1}), followed by Visible Light irradiation for 60 min. To evaluate the effect of irradiation time, 200 mg of materials was added to 25 mL of MB solution (50 mg L^{-1}), and aliquots were collected at predetermined time intervals (0–125 min). The influence of initial dye concentration was examined using MB solutions with concentrations ranging from 10 to 50 mg L^{-1} (20 mL) in the presence of 200 mg of materials, under Visible Light irradiation for 60 min. The residual MB concentration was determined using a UV–Vis spectrophotometer at the maximum absorption wavelength of 665 nm.

3. RESULTS AND DISCUSSION

3.1 Characteristic of Materials

The raw rice husk was successfully prepared under a continuous flow of N_2 gas to enhance the generation and transport of pyrolysis vapours within the reactor. The primary function of N_2 gas is to remove oxygen from the reactor, thereby ensuring that the pyrolysis process occurs under inert conditions. The pyrolysis temperature was set at 500°C. According to Hidayat et al. (2023); Palapa et al. (2023) at a pyrolysis temperature of 550°C, the SiO_2 concentration exceeds 89.47%, and higher temperatures further promote the formation of silicate compounds. This phenomenon is attributed to the use of biomass containing a high proportion of amorphous silicon, where pyrolysis within the temperature range of 250–350°C can induce cracking of the carbon layers in the C−Si−C structure of the biomass, thereby increasing the solubility of silicon in the resulting biochar (Bc). Then, Bnt-Bc was successfully synthesized by

impregnation method. The obtained materials as the starting material were characterized using FTIR, XRD, surface area by BET method, UV-Drs and SEM analyses.

Table 1. Surface Properties of Materials

Materials	Surface Area	Pore Size
Biochar (Bc)	2.5377 m^2/g	878.4045 Å
Bentonite (Bnt)	90.6243 m^2/g	46.8661 Å
Bentonite-Biochar (Bnt-Bc)	13.1459 m^2/g	166.6582 Å

The N_2 adsorption–desorption isotherms and pore size distribution profiles (Figure 1c) reveal distinct textural differences among bentonite (Bnt), biochar (Bc), and the Bnt–Bc composite. All samples exhibit type IV isotherms with pronounced hysteresis loops at P/P_0 >0.4, confirming the predominance of mesoporous structures. According to the BET results (Table 1), biochar incorporation significantly modifies the pore architecture, resulting in an approximately sixfold increase in specific surface area compared to the pristine material. Bentonite shows high nitrogen uptake over the entire relative pressure range, particularly at P/P_0 >0.5, due to its layered structure and well-developed interlayer porosity. In contrast, biochar presents limited adsorption at low and intermediate P/P_0, followed by a sharp increase near P/P_0 = 0.9–1.0, indicating the presence of larger meso- and macropores formed during pyrolysis (Dira et al., 2026). The Bnt–Bc composite displays intermediate adsorption behaviour, suggesting a synergistic pore structure; however, the reduced adsorption relative to pristine bentonite indicates partial blockage of interlayer spaces by biochar, leading to decreased accessibility of bentonite-derived surface area. Similar findings by Ramesh and Raghavan (2025) that the interlayer of bentonite was intercalated by biochar. However, this intercalation simultaneously promotes pore widening and the formation of new mesoporous channels.

X-ray diffraction (XRD) analysis was performed to investigate the phase composition and structural properties of bentonite (Bnt), rice husk–derived biochar (Bc), and the Bnt–Bc composite (Figure 1a). The diffraction patterns of Bnt and Bnt–Bc are dominated by broad reflections, indicating predominantly amorphous or poorly crystalline structures typical of clay–carbon composites. Characteristic bentonite peaks appear at 2θ = 10° (001), 20.07° (003), and 60° (110), confirming its layered structure. The basal spacing (d_{001}), calculated using Bragg's law, is approximately 0.88 nm for pristine bentonite, consistent with montmorillonite-type clays (Salah et al., 2025). After biochar incorporation, the (001) peak shifts to lower intensity with a reduced d-spacing (Sun et al., 2021), suggesting partial occupation or collapse of interlayer galleries due to biochar intercalation bentonite (Dhar et al., 2023; Hass Caetano Lacerda et al., 2020). The composite also exhibits a peak at 2θ = 26.66°, assigned to crystalline SiO_2 from rice husk ash, along with a broad band around 24° corresponding to turbostratic carbon, indicating a disordered graphitic structure (Ajayi et al., 2021). These structural modifications correlate well with BET results, where partial interlayer blockage and lamellar disruption contribute to altered porosity and the development of a hierarchical pore system in the Bnt–Bc composite.

Thus, Figure 1b. showed that FTIR spectroscopy was used to identify surface functional groups and to elucidate adsorption-related interactions in biochar (Bc), bentonite (Bnt), and the biochar–bentonite composite (Bnt–Bc). A broad band at 3600–3200 cm^{-1}, attributed to –OH stretching of structural hydroxyls and adsorbed water, is more pronounced in Bnt and becomes broader in Bnt–Bc, indicating enhanced hydrogen bonding between oxygenated biochar groups and bentonite surfaces. The presence of aliphatic C–H stretching bands at 2920–2850 cm^{-1} confirms the retention of biochar-derived organic functionalities in the composite (Aziz et al., 2023). The band near 1630–1650 cm^{-1}, associated with H–O–H bending and C=O stretching, suggests increased surface polarity, favouring electrostatic interactions with charged adsorbates. Strong Si–O–Si and Si–O–Al stretching vibrations at 1040–1000 cm^{-1} remain evident in Bnt–Bc, indicating preserved clay frameworks, while reduced intensity implies interlayer modification.

The optical properties of the materials are presented in Figures 1(d) and 1(e). Figure 1(d) illustrates the Tauc plots used to estimate the optical band gap energies of both samples. The band gap of pristine bentonite (Bnt) was determined to be approximately 1.15 eV, whereas the Bnt–Bc composite exhibited an increased band gap of about 1.66 eV. This enlargement of the band gap suggests that incorporation of rice husk biochar modifies the electronic structure of bentonite, promoting more efficient electron excitation from the valence band to the conduction band under visible-light irradiation. Consequently, this modification enhances light-harvesting capability and improves the potential Adsorption–Photocatalytic Degradation performance of the composite material.

Figure 1(e) shows the UV–Vis diffuse reflectance spectra (DRS) of Bnt and Bnt–Bc. Both materials display absorption in both the UV and visible regions, suggesting their capability to be activated under visible-light irradiation. However, pristine Bnt displays a higher absorption intensity, particularly characterized by broad absorption bands in the visible region (Priatna et al., 2024). Despite this, the incorporation of biochar broadens the overall absorption range of the composite, which may facilitate improved utilization of the solar spectrum. The observed absorption behaviour suggests that silica-based components in bentonite contribute to photoactive semiconductor characteristics, while the addition of biochar enhances light absorption across a wider wavelength range, thereby potentially strengthening photocatalytic activity (Abdu et al., 2025; Darmawan et al., 2025). The UV-region absorption bands are associated with functional groups within the biochar matrix, which facilitate photo-induced interactions in the composite system.

Figure 2 presents the SEM micrographs of Bnt, Bc, and the Bnt–Bc composite. Pristine bentonite (Bnt) exhibits a characteristic layered, plate-like morphology with stacked lamellar

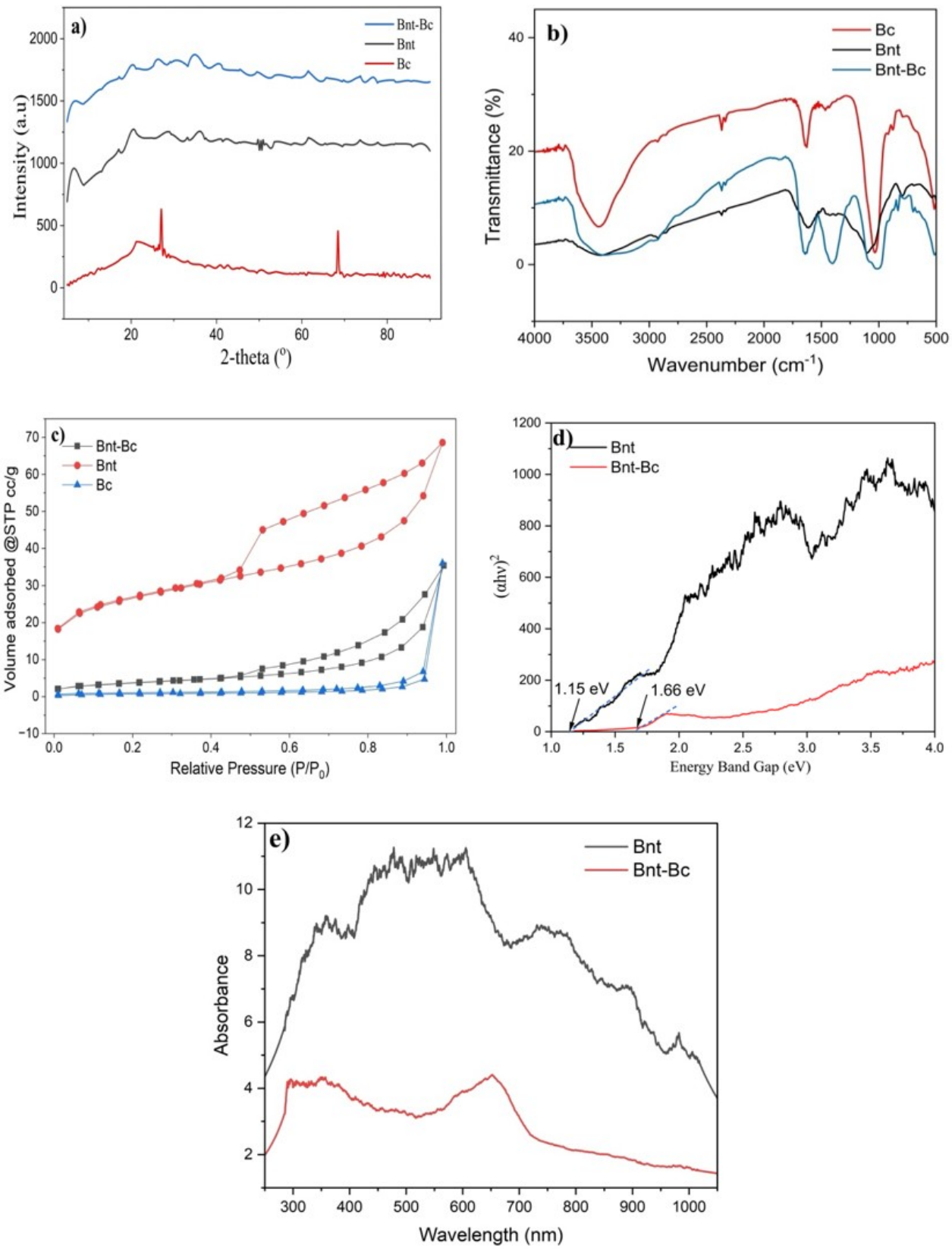

Figure 1. XRD Pattern (a), FTIR Diffraction (b), Adsorption-Desorption N_2 (c), Tauc Plot of Materials (d), and UV DRS Spectrum (e)

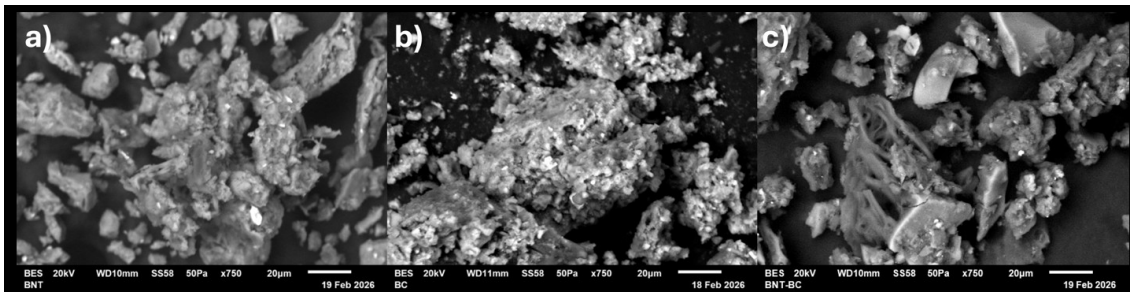

Figure 2. SEM Images of Bnt a), Bc b), and Bnt-Bc c)

sheets forming dense and compact agglomerates, indicative of strong interparticle interactions and limited visible microporosity (Boostani et al., 2025; Rupngam et al., 2025). In contrast, biochar (Bc) shows a highly heterogeneous and fragmented structure with a rough surface texture, loosely packed particles, and evident voids and cavities, reflecting the porous carbonaceous framework generated during pyrolysis (Rupngam et al., 2025). The BNT–BC composite displays integrated morphological features of both components, where the lamellar clay structure remains discernible but is partially covered and interspersed with irregular biochar fragments. This incorporation results in a less compact structure with increased surface roughness and more open architecture, suggesting improved textural properties that may enhance surface reactivity and mass transfer performance (Dira et al., 2026).

3.2 Evaluation of Methylene Blue Removal under Visible Light Irradiation

The performance of bentonite (Bnt), biochar (Bc), and the biochar–bentonite composite (Bnt–Bc) was evaluated under irradiation, as shown in Figure 3. Figure 3(a) presents the temporal evolution of the normalized concentration (C/C_0). The Bnt–Bc composite exhibits the most pronounced decrease in C/C_0 over time, reaching values below 0.15 after 150 min, whereas pristine bentonite shows a relatively limited removal efficiency. This similar findings by Sun et al. (2021) that the biochar displays rapid initial removal and showed good performance for photocatalytic. The kinetics were further analysed using a pseudo-first-order model, $\ln(C/C_0) = -kt$ (Figure 3(b)). The apparent rate constant (k) of Bnt–Bc (0.0034 min^{-1}, R^2 = 0.8691) is higher than that of bentonite (0.0019 min^{-1}, R^2 = 0.7416), confirming the superior photocatalytic activity of the composite. Although biochar exhibits a higher apparent slope (0.0106 min^{-1}), its lower linearity suggests that the photocatalytic degradation was reached equilibrium earlier.

Figure 3(c) illustrates the effect of catalyst dosage. The Bnt–Bc composite achieves high removal efficiency (>85%) at relatively low mass loadings and maintains stable performance up to 200 mg, whereas bentonite shows a declining trend due to light scattering and limited active sites. The consistently high efficiency of Bnt–Bc indicates improved light utilization and enhanced accessibility of reactive sites.

As shown in Figure 3(d), the Bnt–Bc composite demonstrates the highest efficiency across the tested concentration range (50–100), achieving up to 98% removal. This superior performance is attributed to synergistic effects between biochar and bentonite, including enhanced removal capacity, improved charge separation, and increased availability of surface functional groups, in agreement with BET, XRD, and FTIR analyses.

Table 2 summarizes the Adsorption–Photocatalytic Degradation of methylene blue using various materials reported in the literature and compares them with the -Bc composite developed in this study. Conventional semiconductor photocatalysts such as metal oxide exhibit high degradation efficiencies; however, their performance is often limited by UV-light dependency, particle agglomeration, and poor recyclability (Behnajady et al., 2006; Janani et al., 2021; MacHale et al., 2021). Carbon-based materials such as pristine biochar primarily rely on adsorption rather than true photocatalytic degradation, resulting in high initial removal but limited mineralization (Yontar et al., 2022).

The FTIR spectra of fresh and used Bnt–Bc are presented in Figure 4. The absorption band around 1400 cm^{-1} can be attributed to conjugated hydrocarbon carbonyl groups and N–H bonds observed in the composite after Visible Light irradiation, while the peak at 1102 cm^{-1} corresponds to –C–O–H stretching vibrations (Obaideen et al., 2025). A significant change in the absorption intensity associated with silanol (Si–OH) groups is observed compared to that of the C–O functional groups, suggesting that silanol groups play a more dominant role in the adsorption process than carbonyl-related functionalities (Ren et al., 2025).

3.3 Reusability Test

The reusability performance of the catalysts demonstrates distinct stability trends over consecutive cycles (as shown in Figure 5). Pristine bentonite (Bnt) exhibits moderate initial degradation efficiency (77.06%) but rapidly loses activity after the first cycle, indicating limited structural stability and active site durability. In contrast, biochar (Bc) maintains high degradation efficiency across four cycles, decreasing only slightly from 91.42% to 77.09%, reflecting its superior structural robustness and resistance to deactivation. The Bnt-Bc composite shows

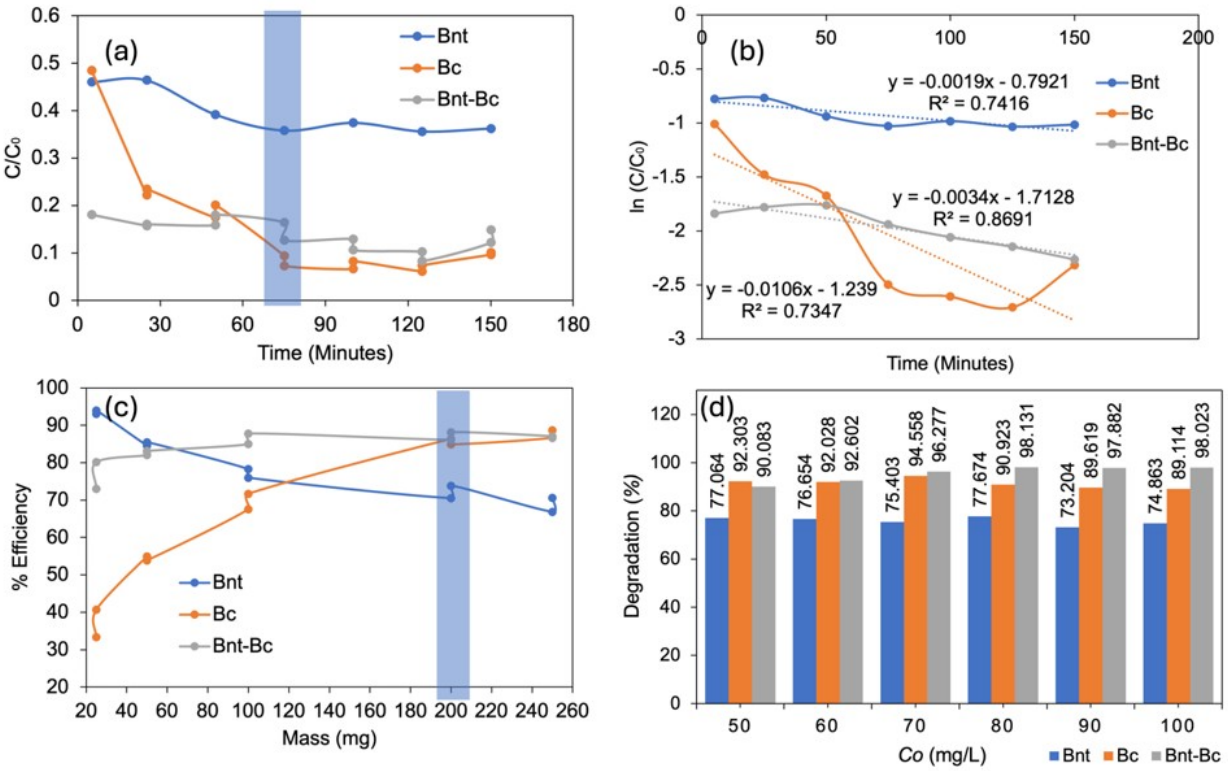

Figure 3. Adsorption–Photocatalytic Degradation of MB on the Materials, (a) Irradiation Time Change (b) 1st-Order Kinetic Linear Fit (c) Effect of the Amount (d) Effect of MB Concentration

Table 2. Comparison of MB Photocatalysis by Several Treatments

Materials	Methods	Results	References
Bentonite	UV irradiation	~85–90% MB removal within 60 min; pH 4	(Banat et al., 2009)
ZnO nanoparticles	UV light-assisted photocatalysis	~88% degradation in 90 min; limited stability	(Behnajady et al., 2006)
g-C_3N_4	Visible-light photocatalysis	~75–80% degradation in 120 min; low surface area	(Masri et al., 2025)
Biochar	Adsorption + pseudo-photocatalysis	~70–85% MB removal; adsorption-dominated	(Dhila et al., 2025)
TiO_2/ExG	Photocatalytic activity	TiO_2/ExG (70.7%) after 2 hours of UV exposure	(Jain et al., 2024)
Bentonite	Adsorption-assisted process	~65–75% MB removal; no true photocatalysis	(Dhar et al., 2023)
Biochar/TiO_2 composite	UV-Vis photocatalysis	>90% MB degradation; improved charge separation	(Bopape, 2026)
Clay-based composite (Bentonite/oxide)	UV photocatalysis	~80–90% degradation; moderate kinetics	(Banat et al., 2009)
LDH-POM	UV photocatalysis	80–90% MB degradation	(Hanifah and Ahmad, 2025)
Biochar–Bentonite (this work)	Adsorption–photocatalysis synergy	~98% MB removal within 150 min; $k \approx 0.0034$ min^{-1}; high stability	This study

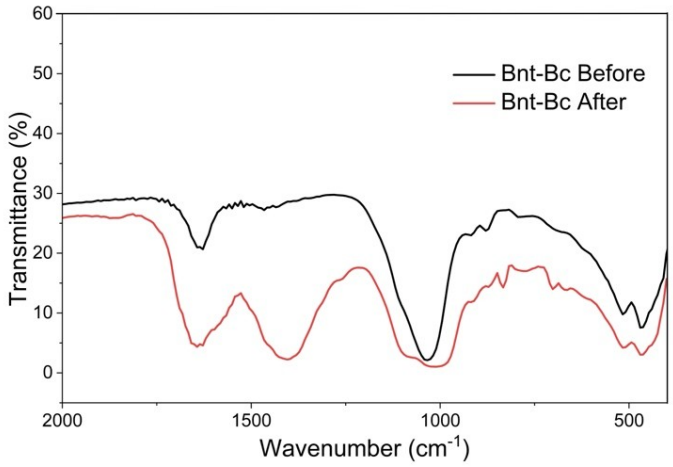

Figure 4. FTIR Analysis Spectra for Composite Before and After Photodegradation

intermediate behaviour, with degradation efficiency declining progressively from 82.20% to 27.12% after the fourth cycle, suggesting partial loss of active sites and possible surface fouling during repeated use.

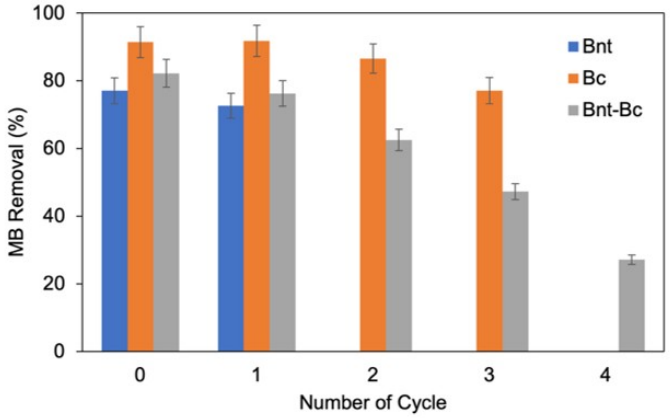

Figure 5. Reusability Performance of the Materials Over Successive Cycles

The enhanced recyclability of Bc and the improved initial stability of the composite can be attributed to the porous carbon framework and improved interfacial interactions, which facilitate mass transfer and mitigate catalyst deactivation, as widely reported for biochar-based and clay–carbon composite photocatalysts in recent studies (Zhang et al., 2026; Chen et al., 2011; Li et al., 2023; Wang et al., 2022). Overall, these findings indicate that biochar incorporation enhances catalyst durability, although further optimization is required to improve long-term stability of the composite system.

The mechanism of methylene blue (MB) removal over the Bnt–Bc composite under visible light irradiation is presented in Figure 6. UV–DRS analysis indicates a band gap of approximately 1.66 eV, confirming that the material can be activated by visible light. When exposed to irradiation ($h\nu \geq E_g$), electrons are promoted from the valence band (VB) to the conduction band (CB), leading to the formation of electron–hole (e^-/h^+) pairs (Shu et al., 2023). The excited electrons subsequently interact with dissolved oxygen to generate superoxide radicals ($\cdot O_2^-$), while the photogenerated holes react with water molecules to produce hydroxyl radicals (·OH. These reactive oxygen species contribute to the degradation of MB molecules adsorbed on the composite surface into intermediate compounds and eventually less harmful end products (Alburaih et al., 2023). The improved removal performance is associated with the complementary functions of bentonite, which offers abundant adsorption sites, and biochar, which enhances charge transport and reduces electron–hole recombination, thereby promoting more efficient removal under visible light irradiation.

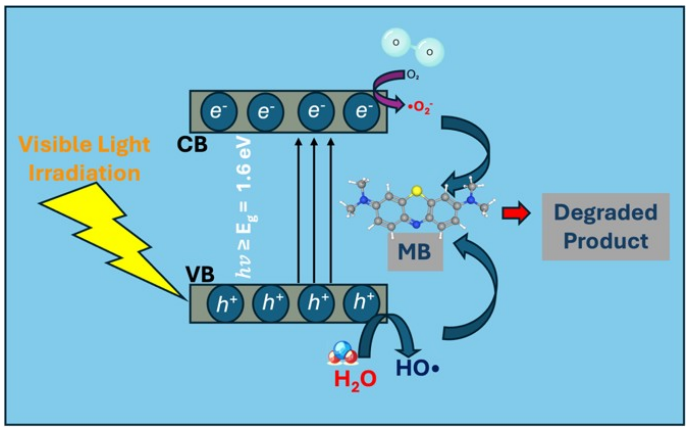

Figure 6. Sketch of the Mechanism of Photocatalytic Activity

4. CONCLUSIONS

A bentonite–biochar composite (Bnt–Bc) was successfully prepared using rice husk–derived biochar and evaluated for photocatalytic degradation of methylene blue. XRD analysis confirmed partial modification of bentonite interlayer spacing after biochar incorporation, while BET results revealed pore enlargement and redistribution, leading to improved accessibility of active sites. FTIR spectra indicated the presence of abundant oxygen-containing functional groups, supporting adsorption mechanisms dominated by hydrogen bonding, electrostatic attraction, and cation exchange. Photocatalytic experiments demonstrated that the Bnt–Bc composite achieved a high MB removal efficiency of approximately 98%, outperforming pristine bentonite and biochar. The enhanced performance arises from the synergistic interaction between adsorption and photo-assisted degradation, rather than conventional semiconductor-driven photocatalysis. These findings highlight the potential of clay–biochar composites as cost-effective, environmentally friendly materials for dye-contaminated wastewater treatment and provide a promising alternative to traditional photocatalysts.

5. ACKNOWLEDGMENT

The authors gratefully acknowledge the Inorganic Chemistry Laboratory, Faculty of Mathematics and Natural Sciences, for providing analytical support. The authors also thank the Advanced Chemical Characterization Laboratory, National Research and Innovation Agency (BRIN), for technical assistance through the E-Layanan Sains program.

REFERENCES

Abdu, M., A. Worku, S. Babaee, P. Diale, T. A. Msagati, and J. F. Nure (2025). The Development of TiO_2-Biochar Composite Material for Photodegradation of Basic Blue 41 and Erichrome Black T Azo Dyes from Water. *Surfaces and Interfaces*, **62**; 106156

Ajayi, O. A., O. O. Okeniyi, O. A. Adekunle, and Y. M. Sani (2021). Development and Characterization of Rice Husk Ash-Based Photocatalyst for Degradation of Methylene Blue. *Journal of Materials and Environmental Science*; 1360–1372

Alburaih, H. A., S. Aman, N. Ahmad, S. R. Ejaz, R. Y. Khosa, A. G. Abid, S. Manzoor, H. M. T. Farid, M. S. Waheed, and T. A. Taha (2023). Synergistic Photodegradation of Methylene Blue by Sm-Doped Fe_2O_3 Photocatalyst Under Sunlight. *Chinese Journal of Physics*, **83**; 637–649

Ashamary, F., P. C. Neba, S. Harivarsha, A. Raji, P. Annamalai, M. G. Mohamed, P. Kalambate, P. Muthirulan, S. W. Kuo, and D. Manoj (2025). In Situ Synthesis of 3D ZIF-8 on 2D MXene Nanosheets for Efficient Photocatalytic Degradation of Methylene Blue (MB). *Materials Advances*, **6**; 4660–4671

Aziz, S., B. Uzair, M. I. Ali, S. Anbreen, F. Umber, M. Khalid, A. A. Aljabali, Y. Mishra, V. Mishra, Á. Serrano-Aroca, G. A. Naikoo, M. El-Tanani, S. Haque, A. G. Almutary, and M. M. Tambuwala (2023). Synthesis and Characterization of Nanobiochar from Rice Husk Biochar for the Removal of Safranin and Malachite Green from Water. *Environmental Research*, **238**; 116909

Banat, F., S. Al-Asheh, R. Zomaout, B. Qtaishat, T. Alateat, and S. Almayta (2009). Photodegradation of Methylene Blue Dye Using Bentonite as a Catalyst. *Desalination and Water Treatment*, **5**; 283–289

Behnajady, M. A., N. Modirshahla, and R. Hamzavi (2006). Kinetic Study on Photocatalytic Degradation of C.I. Acid Yellow 23 by ZnO Photocatalyst. *Journal of Hazardous Materials*, **133**; 226–232

Boostani, H. R., Z. Jalalpour, A. Behpouri, E. Bijanzadeh, and M. Najafi-Ghiri (2025). Comparative Efficacy of Individually and Combined Application of Compost, Biochar, and Bentonite on Ni Dynamics in a Calcareous Soil. *SOIL*, **11**; 939–955

Bopape, D. A. (2026). Exploring the Synthesis and Application of ZnO-, TiO_2-, CuO-ZnO- and CuO-TiO_2 Carbon Sphere (CSs) Nanocomposites for the Photocatalytic Degradation of Methylene Blue (MB) Dye and Ciprofloxacin (CIP) Antibiotic Under Ultraviolet (UV) Irradiation. *Journal of Water Process Engineering*, **81**; 109392

Chakrabarti, S. and B. K. Dutta (2004). Photocatalytic Degradation of Model Textile Dyes in Wastewater Using ZnO as Semiconductor Catalyst. *Journal of Hazardous Materials*, **112**; 269–278

Chen, Z.-x., X.-y. Jin, Z. Chen, M. Megharaj, and R. Naidu (2011). Removal of Methyl Orange from Aqueous Solution Using Bentonite-Supported Nanoscale Zero-valent Iron. *Journal of Colloid and Interface Science*, **363**(2); 601–607

Darmawan, A., D. A. Batu Bara, M. Al Fahmi, H. Muhtar, and D. N. Bima (2025). Synergistic Photodegradation of Remazol Black B Dye Using Sulfur-Doped g-C_3N_4/rGO Composite: The Dual Role of Thiourea. *Journal of Water Process Engineering*, **72**; 107545

Dhar, A. K., H. A. Himu, M. Bhattacharjee, M. G. Mostufa, and F. Parvin (2023). Insights on Applications of Bentonite Clays for the Removal of Dyes and Heavy Metals from Wastewater: A Review. *Environmental Science and Pollution Research*, **30**; 5440–5474

Dhila, H., A. Bhapkar, and S. Bhame (2025). Metal Oxide/Biochar Hybrid Nanocomposites for Adsorption and Photocatalytic Degradation of Textile Dye Effluents: A Review. *Desalination and Water Treatment*, **321**; 101004

Dira, A., A. Ayad, A. Harrou, A. Elmouwahidi, F. Carrasco-Marin, and E. Gharibi (2026). Insight into the Synergistic Adsorption Mechanism of a Novel Biochar-Bentonite Composite for Malachite Green Removal: A DFT-Guided Study. *Journal of Water Process Engineering*, **83**; 109623

Gnanamozhi, P., A. Monamary, S. D. Jereil, J. E. Pauline, J. A. O. Ratnam, A. Ganeshkumar, V. Pandiyan, A. A. Alothman, R. A. Alshgari, and M. Govindasamy (2023). Effective Photocatalytic Degradation of Methylene Blue (MB) and Reactive Red 120 (RR120) Using Al-Substituted ZnO Nanoparticles. *Surfaces and Interfaces*, **41**; 103203

Hanifah, Y. and N. Ahmad (2025). Polyoxometalate-Assisted Layered Double Hydroxide for Facile Photocatalytic Methylene Blue and Malachite Green. *Science and Technology Indonesia*, **10**; 1312–1321

Hass Caetano Lacerda, E., F. C. Monteiro, J. R. Kloss, and S. T. Fujiwara (2020). Bentonite Clay Modified with Nb_2O_5: An Efficient and Reused Photocatalyst for the Degradation of Reactive Textile Dye. *Journal of Photochemistry and Photobiology A: Chemistry*, **388**; 112084

Hidayat, A. Rahmat, R. C. Nissa, Sukamto, L. Nuraini, M. Nurtanto, and W. S. Ramadhani (2023). Analysis of Rice Husk Biochar Characteristics Under Different Pyrolysis Temperature. In *IOP Conference Series: Earth and Environmental Science*, volume 1201. page 012095

Jain, R., M. Upadhyaya, A. Singh, and R. P. Jaiswal (2024). TiO_2 Nanoparticles Synthesized on Graphene Nanosheets with Varied Crystallinity for Photocatalytic Degradation of MB Dye. *Journal of Environmental Chemical Engineering*, **12**; 113881

Janani, F. Z., H. Khiar, N. Taoufik, A. Elhalil, M. Sadiq, A. V. Puga, S. Mansouri, and N. Barka (2021). ZnO–Al_2O_3–CeO_2–Ce_2O_3 Mixed Metal Oxides as a

Promising Photocatalyst for Methyl Orange Photocatalytic Degradation. *Materials Today Chemistry*, **21**; 100495

Kambo, H. S. and A. Dutta (2015). A Comparative Review of Biochar and Hydrochar in Terms of Production, Physico-Chemical Properties and Applications. *Renewable and Sustainable Energy Reviews*, (45); 359–378

Li, L., Z. Yin, M. Cheng, L. Qin, S. Liu, H. Yi, M. Zhang, Y. Fu, X. Yang, X. Zhou, et al. (2023). Insights into Reactive Species Generation and Organics Selective Degradation in Fe-Based Heterogeneous Fenton-like Systems: A Critical Review. *Chemical Engineering Journal*, **454**; 140126

Liu, S. Z., W. Ding, H. W. Zhang, Z. S. Li, K. C. Tian, C. Liu, Z. C. Geng, and C. Y. Xu (2024). Magnetized Bentonite Modified Rice Straw Biochar: Qualitative and Quantitative Analysis of Cd(II) Adsorption Mechanism. *Chemosphere*, **359**; 142262

MacHale, A. R., S. A. Phaltane, H. D. Shelke, and L. D. Kadam (2021). Facile Hydrothermal Synthesis of Cu_2SnS_3 Nanoparticles for Photocatalytic Dye Degradation of Methylene Blue. *Materials Today Proceedings*, **43**; 2768–2773

Masri, M., G. K. B, A. Hezam, K. Alkanad, T. F. Qahtan, Q. A. Drmosh, F. Masri, K. Prashantha, M. S. H, S. M. Abdu Kaid, Udayabhanu, and K. Byrappa (2025). Boosting the Photocatalytic Efficiency of g-C_3N_4 for Effective Removal of RhB and MB from Aqueous Medium. *Colloids and Surfaces C: Environmental Aspects*, **3**; 100074

Obaideen, K., N. Shehata, E. T. Sayed, M. A. Abdelkareem, M. S. Mahmoud, and A. G. Olabi (2025). Synergistic Adsorption-Photocatalytic Remediation of Methylene Blue Dye from Textile Industry Wastewater over NiFe LDH Supported on Tyre-Ash Derived Activated Carbon. *Applied Surface Science*, **679**; 161205

Palapa, N. R., A. Amri, and Y. Hanifah (2023). Potential Indonesian Rice Husk for Wastewater Treatment Agricultural Waste Preparation and Dye Removal Application. *Indonesian Journal of Environmental Management and Sustainability*, **7**; 160–165

Priatna, S. J., A. Yuliana, Zulkarnain, E. Melwita, F. S. Arsyad, and R. Mohadi (2024). Removal of Methyl Orange in Aqueous Medium Using ZnO/Bentonite as Semiconductor by Photocatalytic Process. *Science and Technology Indonesia*, **9**; 539–545

Qian, X., H. Han, Y. Chen, and Y. Yuan (2018). Sol–Gel Solvothermal Route to Synthesize Anatase/Brookite/Rutile TiO_2 Nanocomposites with Highly Photocatalytic Activity. *Journal of Sol-Gel Science and Technology*, **85**; 394–401

Ramesh, K. and V. Raghavan (2025). Biochar/Bentonite Composite Beads for Controlled Nitrogen Release and Reduced Environmental Impact: From Banana Waste to Sustainable Food Security. *Results in Surfaces and Interfaces*, **19**; 100500

Ren, H., G. Long, Y. Chen, Y. Gao, H. Mao, X. Gong, D. Xue, G. Hu, and B. Wang (2025). Enhanced Methylene Blue Degradation by Graphene Oxide-Encapsulated Nano Zero-Valent Iron Composites: Optimization, Mechanistic Insights, and Environmental Implications. *Materials Science in Semiconductor Processing*, **185**; 108869

Rupngam, T., P. Udomkun, T. Boonupara, and P. Kaewlom (2025). Contrasting Pre- and Post-Pyrolysis Incorporation of Bentonite into Manure Biochar: Impacts on Nutrient Availability, Carbon Stability, and Physicochemical Properties. *Agronomy*, **15**(8); 2015

Salah, M. M., M. S. Hammad, A. L. Fayed, and A. M. Ebid (2025). The Influence of Bentonite Content on the Properties of Its Mixture with Kaolinite. *Scientific Reports*, **15**; 10982

Saravanan, R., S. Karthikeyan, V. K. Gupta, G. Sekaran, V. Narayanan, and A. Stephen (2013). Enhanced Photocatalytic Activity of ZnO/CuO Nanocomposite for the Degradation of Textile Dye on Visible Light Illumination. *Materials Science and Engineering C*, **33**; 91–98

Sewu, D. D., D. S. Lee, H. N. Tran, and S. H. Woo (2019). Effect of Bentonite-Mineral Co-Pyrolysis with Macroalgae on Physicochemical Property and Dye Uptake Capacity of Bentonite/Biochar Composite. *Journal of the Taiwan Institute of Chemical Engineers*, **104**; 106–113

Shu, J., K. Wang, V. K. Sharma, X. Xu, N. Nesnas, and H. Wang (2023). Efficient Micropollutants Degradation by Ferrate(VI)-Ti/Zn LDH Composite under Visible Light: Activation of Ferrate(VI) and Self-Formation of Fe(III)-LDH Heterojunction. *Chemical Engineering Journal*, **456**; 141127

Sun, W., H. Zeng, and T. Tang (2021). Enhanced Adsorption of Anionic Polymer on Montmorillonite by Divalent Cations and the Effect of Salinity. *Journal of Physical Chemistry A*, **125**; 1025–1035

Wang, W., Q. Dong, H. Qiu, H. Li, Y. Mao, Y. Liu, T. Gong, M. Xiang, Y. Huang, C. Wang, et al. (2022). Rapid Reactivation of Aged NZVI/GO by *Shewanella* CN32 for Efficient Removal of Tetrabromobisphenol A and Associated Reaction Mechanisms. *Journal of Cleaner Production*, **333**; 130215

Xu, D. and H. Ma (2021). Degradation of Rhodamine B in Water by Ultrasound-Assisted TiO_2 Photocatalysis. *Journal of Cleaner Production*, **313**; 127758

Yontar, A. K., S. Avcioğlu, and S. Çevik (2022). Nature-Based Nanocomposites for Adsorption and Visible Light Photocatalytic Degradation of Methylene Blue Dye. *Journal of Cleaner Production*, **380**; 135070

Zahara, Z. A., I. Royani, N. R. Palapa, R. Mohadi, and A. Lesbani (2023). Treatment of Methylene Blue Using Ni-Al/Magnetite Biochar Layered Double Hydroxides Composite by Adsorption. *Bulletin of Chemical Reaction Engineering and Catalysis*, **18**; 659–674

Zhang, P., Z. Shen, L. Jia, and J. Qiu (2026). Biomass-Derived Carbon for Boosting Photocatalysis. *Small*, **22**(8); e12210

Zhao, Y., J. Yao, N. Min, B. Ma, W. Chai, and Y. Ma (2026). Efficient Removal of Cu^{2+}, Pb^{2+}, and Cd^{2+} by Two Magnetic Biochar-Montmorillonite Composites and the Application in Synthetic Wastewater. *Separation and Purification Technology*; 136996

Zhou, B., J. J. Wang, P. Dangal, S. Lomnicki, A. D. Roy, and J. H. Park (2024). A Novel Sugarcane Residue-Derived

Bimetallic Fe/Mn-Biochar Composite for Activation of Peroxymonosulfate in Advanced Oxidation Process Removal of Azo Dye: Degradation Behavior and Mechanism. *Journal of Water Process Engineering*, **58**; 104740